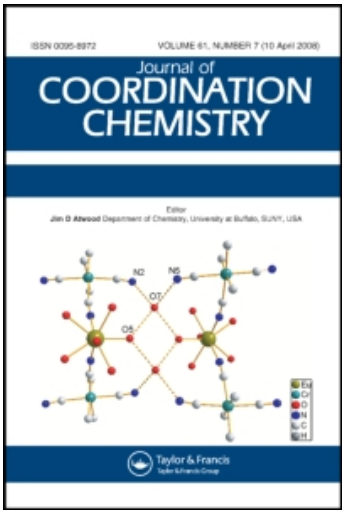

Journal of Coordination Chemistry
Publication details, including instructions for authors and subscription information:
http://www.informaworld.com/smpp/title~content=t713455674

Synthesis of chiral SalenZn(II) and its coordination with imidazole derivatives and amino acid ester derivatives

Ruijuan Yuan[ab]; Wenjuan Ruan[b]; Shujun Wang[b]; Yinghui Zhang[b]; Xiaoli Li[b]; Zhiang Zhu[b]
[a] College of Pharmaceuticals and Biotechnology, Tianjin University, Tianjin 300072, P.R. China [b] Department of Chemistry, Nankai University, Tianjin 300071, P.R. China

To cite this Article Yuan, Ruijuan , Ruan, Wenjuan , Wang, Shujun , Zhang, Yinghui , Li, Xiaoli and Zhu, Zhiang(2006) 'Synthesis of chiral SalenZn(II) and its coordination with imidazole derivatives and amino acid ester derivatives', Journal of Coordination Chemistry, 59: 6, 585 — 595
To link to this Article: DOI: 10.1080/00958970500361130
URL: http://dx.doi.org/10.1080/00958970500361130

Journal of Coordination Chemistry
Vol. 59, No. 6, 15 April 2006, 585–595

Taylor & Francis
Taylor & Francis Group

Synthesis of chiral SalenZn(II) and its coordination with imidazole derivatives and amino acid ester derivatives

RUIJUAN YUAN†‡, WENJUAN RUAN*‡, SHUJUN WANG‡, YINGHUI ZHANG‡, XIAOLI LI‡ and ZHIANG ZHU‡

†College of Pharmaceuticals and Biotechnology, Tianjin University, Tianjin 300072, P.R. China
‡Department of Chemistry, Nankai University, Tianjin 300071, P.R. China

(*Received 20 January 2005; in final form 28 April 2005*)

A chiral complex, SalenZn(II) (**S**), was synthesized and characterized. Its coordination with imidazole derivatives and amino acid ester derivatives was studied by UV-vis spectrophotometric titrations and CD spectroscopy. The binding constants decreased in the order K (Im) > K (2-MeIm) > K (2-Et-4-MeIm) > K (N-MeIm) for imidazole derivatives, and K (AlaOMe) > K (PheOMe) > K (ValOMe) for amino acid ester derivatives with the same configuration and $K_D > K_L$ for amino acid esters with different configuration. CD spectra can quantify the strength of SalenZn(II)-ligand interactions, giving results consistent with the magnitudes of the binding constants. Moreover the minimum energy conformations of the adducts were obtained by simulated annealing, and quantum chemical calculations were performed based on those conformations to explain experimental results at the molecular level.

Keywords: Chiral SalenZn(II); Coordination; UV-vis spectrum; CD spectrum; Quantum chemical calculation

1. Introduction

The use of metal complexes of chiral Salen (N,N-bis-(saliylaldehyde)ethylenediamine) in catalytic asymmetric synthesis has been widespread because of simple preparation, low cost, structural diversity and high enantioselectivity. They are widely used in asymmetric alkene epoxidation [1, 2], acylation [3], asymmetric sulfoxidation [4], asymmetric synthesis of α-amino acids [5], aziridination [6] and hydrolytic kinetic resolution of epoxides [7]. Enantioselectivity was improved by adding small ligands, e.g. phosphoryl ligands [1], quaternary ammonium salts [8], amine [9], pyridine N-oxide [10] etc., which can form adducts with the Salen complexes, but the detailed mechanism is not clear yet. In order to study the interaction of a Salen metal complex with a ligand, a novel chiral SalenZn(II) complex has been synthesized and coordination with imidazole derivatives and amino acid ester derivatives has been studied by UV-vis spectrophotometric titration experiments and CD spectroscopy. Furthermore, the conformations of the adducts

*Corresponding author. Email: wjruan@nankai.edu.cn

Journal of Coordination Chemistry
ISSN 0095-8972 print: ISSN 1029-0389 online © 2006 Taylor & Francis
DOI: 10.1080/00958970500361130

have also been investigated via simulated annealing. The results will be helpful to the mechanism of the catalysis and asymmetric synthesis.

2. Experimental

2.1. *Materials and measurements*

Ligands used in this article include imidazole (Im), 2-methyl-imidazole (2-MeIm), N-methyl-imidazole (N-MeIm), 2-ethyl-4-methyl-imidazole (2-Et-4-Me-Im), *L*- and *D*-alanine methyl ester (*L*- and *D*-AlaOMe), *L*- and *D*-valine methyl ester (*L*- and *D*-ValOMe), *L*- and *D*-phenylalanine methyl ester (*L*- and *D*-PheOMe). Amino acid esters and (*R*, *R*)-diaminocyclohexane were prepared according to the literature [11, 12]. Dry N,N-dimethylformamide was obtained by vacuum distilling over $MgSO_4$. All above mentioned reagents are of commercial reagent grade and were used without further purification.

^{1}H NMR spectra were recorded on a Mercury V× 300 NMR spectrometer and chemical shifts reported relative to an internal standard, Me_4Si. Infrared spectra (KBr pellet) were recorded on a Bio-Rad FTS 135FT-IR spectrometer. Elemental analysis was determined with a Perkin-Elmer 240c elemental analyzer. A Shimadzu-265 spectrophotometer and JASCO-715 spectropolarimeter were applied to record UV-vis spectra and circular dichroism (CD), respectively. Molecular modeling was carried out with Sybyl 6.9 software using the Tripos force field on an SGI Indigo II workstation.

2.2. *Synthesis*

The procedure used to synthesized the chiral Salen and SalenZn(II) complex is outlined in scheme 1.

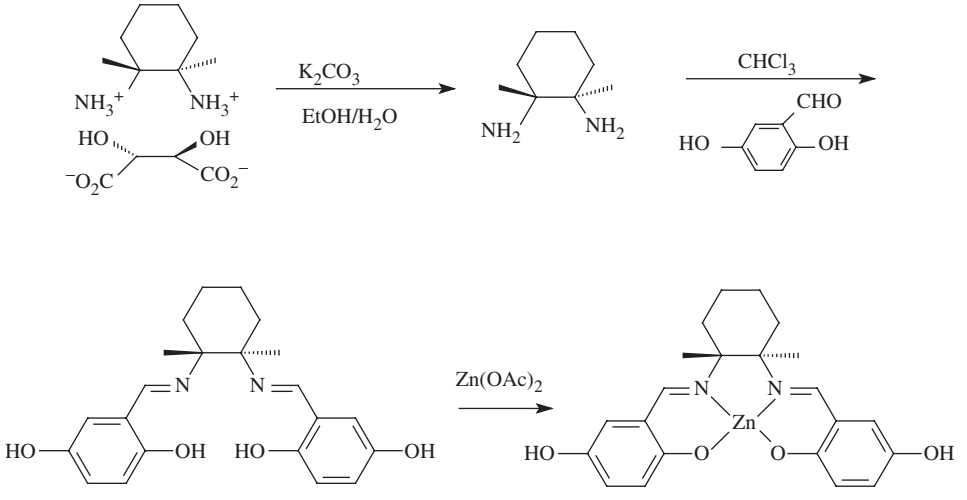

Scheme 1. Synthesis of chiral Salen and SalenZn(II).

Synthesis of chiral Salen ((*R*,*R*)-(-)-*N*,*N*′-bis(5-hydroxylsalicylidene)-1,2-cyclohexanediamino): 2.66 g (10 mmol) of (*R*,*R*)-diaminocyclohexane tartrate, 2.76 g (20 mmol) of potassium carbonate, 20 mL of water and 20 mL of ethanol were added to a 100 mL flask. The mixture was stirred and refluxed for 5 h. After cooling to room temperature, the product was extracted with chloroform and the organic layer was dried using anhydrous Na_2SO_4. After filtration, 0.55 g (4 mmol) of 2,5-dioxyl-benzaldehyde was added to the filtrate and allowed to react at room temperature for 5 h. The solution was condensed and the product was purified on silica gel (ether : petroleum ether = 1 : 1) to obtain the yellow solid product, yield 80%, m.p. 102 ~ 104°C. Anal. Calcd. for $C_{20}H_{22}O_4N_2$(%): C: 67.78, H: 6.26, N: 7.90. Found: C: 67.78, H: 6.34, N: 7.87. ^{1}H NMR ($CDCl_3$) δ (ppm) 8.14 (s, CH=N, 2H), 6.60–7.28 (m, Phenyl, 6H), 3.28–3.31 (m, chiral H, 2H), 0.85–1.95 (m, CH_2, 8H), IR (KBr, pellet) (cm^{-1}) 2932 (m, ν_{C-H}), 2858 (w, ν_{C-H}), 1641 (s, $\nu_{C=N}$), 1591 (s, $\nu_{C=C}$), 1492 (s, $\nu_{C=C}$).

Synthesis of chiral SalenZn(II) ((*R*,*R*)-(-)-*N*,*N*′-bis(5-hydroxylsalicylidene)-1,2-cyclohexane diamino-zinc(II)) (**S**): To a solution of 354 mg (1 mmol) of chiral Salen in 10 mL of methanol a slight excess of $Zn(OAc)_2$ was added. The solution was stirred for 3 h at room temperature. After filtration, the yellow precipitate was washed three times with water, and then dried under vacuum, yield 90%. Anal. Calcd. for $C_{20}H_{20}O_4N_2Zn$(%): C: 57.50, H: 4.83, N: 6.71. Found: C: 57.38, H: 4.88, N: 6.60. IR (KBr, pellet) (cm^{-1}) 3404 (s, ν_{O-H}), 2934 (s, ν_{C-H}), 2859 (s, ν_{C-H}), 1637 (s, $\nu_{C=N}$), 609 (w, ν_{Zn-O}), 539(w, ν_{Zn-N}).

2.3. *UV-vis spectrophotometric titrations*

To a solution of 1×10^{-4} mol dm^{-3} of **S** in DMF a solution of imidazole derivatives or amino acid ester derivatives in DMF was added at room temperature. Changes in the absorbance at 393 nm were monitored at different concentrations of the ligand in the range of $10^{-4} \sim 10^{-2}$ mol dm^{-3}. The ligands are shown in figure 1.

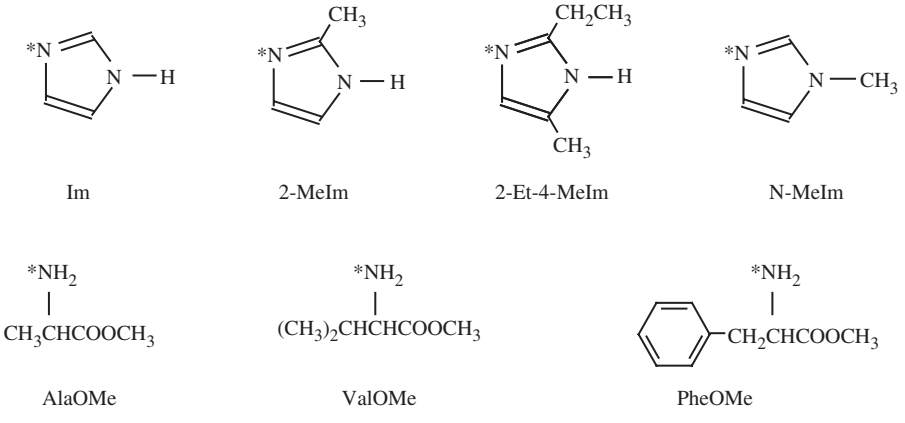

Figure 1. The structure of ligands (the atoms marked with * are the coordinating atoms).

3. Results and discussion

3.1. *UV-vis spectrophotometric titrations*

A representative plot of spectral changes observed upon the addition of Im to **S** is shown in figure 2. With the concentrations of the ligand increasing the absorption peak at 393 nm decreases gradually, while a new absorption peak at 350 nm forms and increases, showing **S** consumption and adduct formation. There is a clear isosbestic point at 370 nm, suggesting that the reaction proceeds cleanly.

The coordination reaction can be expressed as follows:

$$S + nL \overset{K}{\rightleftharpoons} SL_n$$

Where **S** is the chiral SalenZn(II), L is the ligand, n is the coordination number and K is the binding constant. In the presence of a large excess of the ligand (except Im and 2-MeIm) with SalenZn(II) K can be calculated by equation (1) [13]:

$$\frac{A_0}{A_e - A_0} = \frac{\varepsilon_1}{\varepsilon_2 - \varepsilon_1}\frac{1}{Kc_L^n} + \frac{\varepsilon_1}{\varepsilon_2 - \varepsilon_1} \tag{1}$$

Where A_0 is the absorbance of **S** solution, A_e is the equilibrium absorbance in the presence of ligand at concentration c_L, ε_1 and ε_2 are the extinction coefficients of **S** and of the adduct, respectively. The quantity $A_0/(A_e - A_0)$ has a linear relation to $1/c_L$, showing that the coordination number is 1. The binding constant K can be

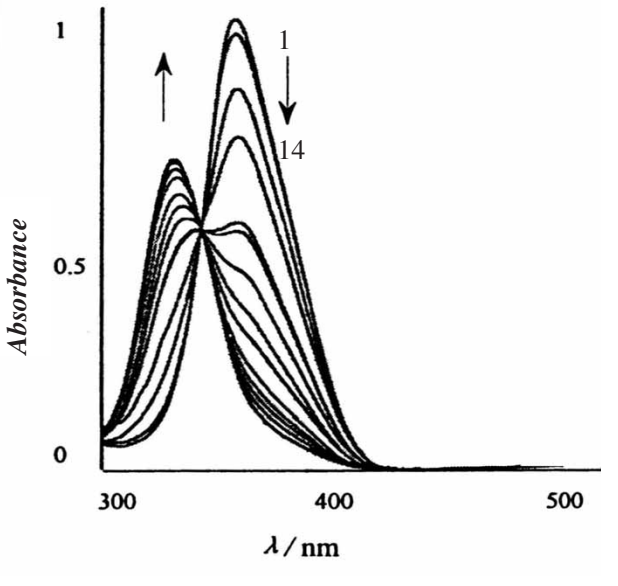

Figure 2. The UV-vis spectra of **S**-Im system (the concentration of **S** is 1×10^{-4} mol l^{-1}, and the concentration ratios of [Im]/[**S**] from 1 ~ 14 are: 0, 5, 1, 1.5, 2, 2.5, 3, 3.5, 4, 4.5, 5, 5.5, 6, 10, respectively).

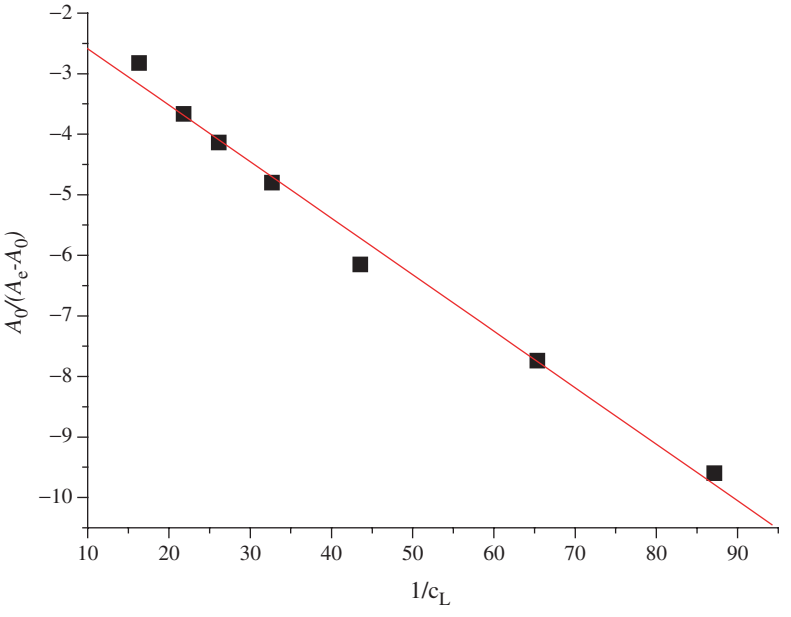

Figure 3. The plot of $A_0/(A_e - A_0)$ *vs.* $1/C_L$ in **S**-*D*-ValOMe system.

Table 1. The binding constants of **S** with imidazole derivatives and with amino acid ester derivatives.

Ligands	$K/(\text{mol}^{-1}\,\text{L})$	Ligands	$K/(\text{mol}^{-1}\,\text{L})$	K_D/K_L
Im	$(6.3 \pm 0.4) \times 10^3$	*D*-AlaOMe	$(2.0 \pm 0.1) \times 10^2$	1.1
2-MeIm	$(3.9 \pm 0.2) \times 10^3$	*L*-AlaOMe	$(1.8 \pm 0.1) \times 10^2$	
2-Et-4-Me-Im	$(5.4 \pm 0.3) \times 10$	*D*-PheOMe	$(3.3 \pm 0.2) \times 10$	1.9
N-MeIm	$(4.0 \pm 0.2) \times 10$	*L*-PheOMe	$(1.7 \pm 0.1) \times 10$	
		D-ValOMe	$(1.7 \pm 0.1) \times 10$	2.1
		L-ValOMe	8.2 ± 0.5	

obtained from the ratio of the intercept to the slope. With a small excess of the ligands Im and 2-MeIm and SalenZn(II), the binding constants K are calculated by the method of Rose and Drago [14]. For the formation of a 1 : 1 adduct,

$$\frac{1}{K} = \frac{(A_e - A_0)}{(\varepsilon_2 - \varepsilon_1) - c_0 - c_L} + c_0 c_L \left[\frac{(\varepsilon_2 - \varepsilon_1)}{(A_e - A_0)}\right] \tag{2}$$

where c_0 and c_L are the concentrations of **S** and the ligand, respectively. For a given solution all the terms of the Rose–Drago equation are known except for $1/K$ and $(\varepsilon_2 - \varepsilon_1)$ which are constants to be determined. To do this, a range of $(\varepsilon_2 - \varepsilon_1)$ values is chosen that will encompass the true value. A plot of $1/K$ versus $\Delta\varepsilon(=\varepsilon_2 - \varepsilon_1)$ for solutions of varying concentrations of ligands gives an intersection point that determines the unique K^{-1}.

A representive plot is shown in figure 3 and the binding constants K are listed in table 1.

Table 2. The net charge value of coordination atom in the ligands.

Axial ligand	Net charge	Axial ligand	Net charge
Im	−0.648772	*L*-AlaOMe	−0.719113
2-MeIm	−0.679015	*D*-AlaOMe	−0.721606
N-MeIm	−0.657460	*L*-PheOMe	−0.736438
2-Et-4-MeIm	−0.695502	*D*-PheOMe	−0.740544
		L-ValOMe	−0.724591
		D-ValOMe	−0.728753

The coordinating capability of the ligand can be affected by many factors, but in this system the main factors which determine the binding affinity of the ligand are steric bulk of the ligand and the net negative charge on the ligand. To consider these two factors, we obtained the net negative charge of coordination atom in the ligands by quantum chemical calculation (table 2).

The larger the absolute value of the net charge of the ligand, the stronger the binding affinity. On the basis of the net charge values given in table 2, the coordinating capability of imidazole derivatives should decrease in the order of 2-Et-4-MeIm > 2-MeIm > N-MeIm > Im. However, steric repulsion hinders ligand approach to **S**, so on the basis of the steric bulk of the ligand, one would expect the binding constants to decrease in the order of Im > N-MeIm > 2-MeIm > 2-Et-4-MeIm. The actual binding constants are in the order Im > 2-MeIm > 2-Et-4-MeIm > N-MeIm because of the combined effect of the two factors.

Amino acid ester derivatives with the same configuration have net charges decreasing in the order PheOMe > ValOMe > AlaOMe, and the steric bulk of the ligands also decreases in the same order. The binding constants listed in table 1 decrease in the order K (AlaOMe) > K (PheOMe) > K (ValOMe), which once again appears to result from the combined effect. For the same amino acid ester with different configuration, the steric bulk is similar. Chiral SalenZn(II) is (*R*,*R*) coordinating preferentially with *D*-amino acid ester, so the binding constants are $K_D > K_L$, consistent with the order of net charge.

3.2. *CD spectrum*

The UV-vis and CD spectra of chiral SalenZn(II) are shown in figure 4(a) and (b), respectively. The absorption peak at 393 nm is induced by the π–π^* transition of C=N which produces a pair of Cotton splits at shorter wavelength 383 nm (+30) and longer wavelength 425 nm (−56) in the CD spectrum. The absorption peak at 282 nm is induced by the π–π^* transition of benzene which produces one negative Cotton split at 270 nm (−30) in the CD spectrum [15]. It is predicted that when the chirality configuration is Λ [16] (IUPAC nomenclature [17]), the negative component of the azomethine π–π^* couplet will lie at higher energy, whereas the lower energy case corresponds to the configuration Δ. (R, R)-Salen metal complexes conform to the Δ configuration [15, 16, 18]. Therefore, the CD spectrum will show a negative Cotton effect at long wavelength.

Figure 5 shows the CD spectra of the **S**-Im system. Although there is a chromophore group of C=N in imidazole, it will not produce a CD signal by itself. However, it will when situated in a chiral environment of **S** because of the distortion of the intrinsic

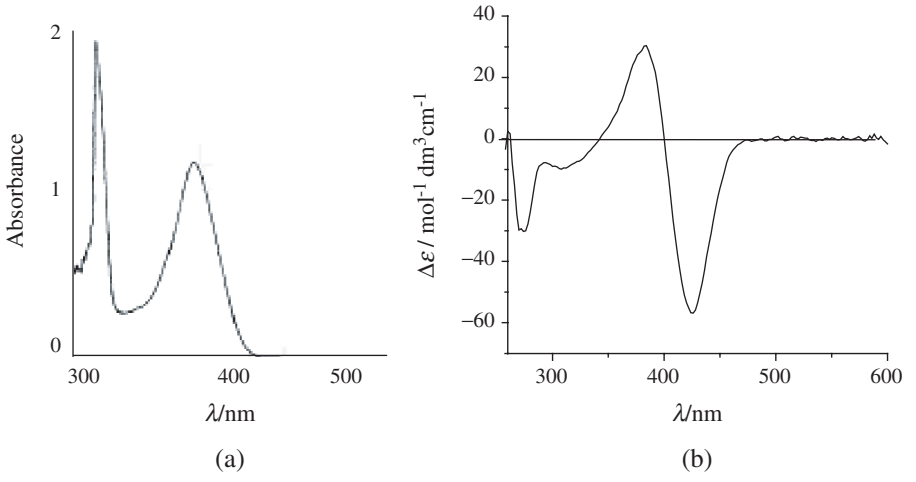

Figure 4. The UV-vis (a) and CD (b) spectra of **S**.

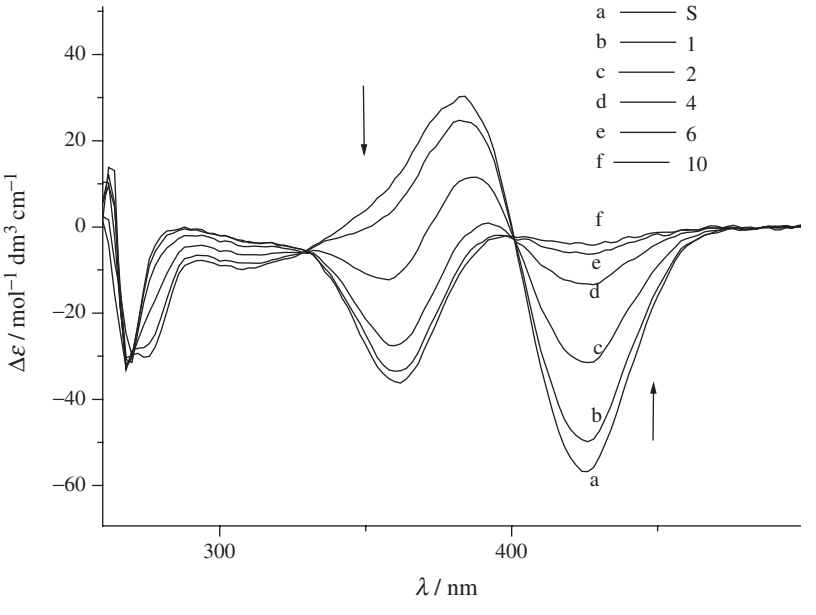

Figure 5. The CD spectra of **S**-Im system (b–f are the concentration ratios of [ligand]/[**S**]).

symmetric chromophore group. From figure 5 it can be observed that the signal intensity of CD spectra at 425 and 383 nm decreases with the increasing concentration of the ligand, while a new signal appears and increases gradually at 360 nm, which is from the adduct. The signal of CD of the adduct moves to shorter wavelength, much like the position of absorption peak of UV-vis spectra moves to shorter wavelength. With regard to other imidazole derivatives, CD spectra are similar.

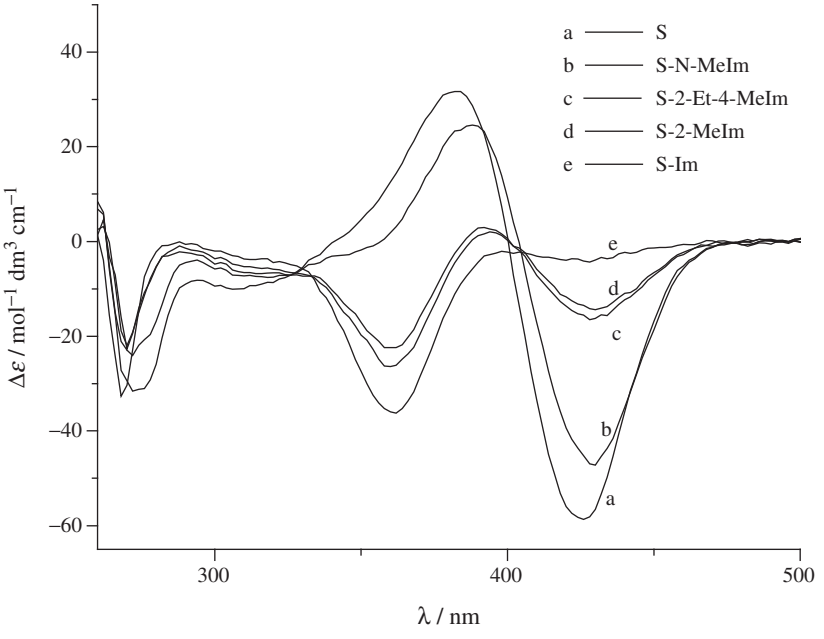

Figure 6. The CD spectra of **S**-imidazole derivatives (the concentrations of ligands are equivalent).

The CD spectra of the system of **S** with imidazole derivatives of the same concentration are illustrated in figure 6. Different CD signal intensities present different coordinating capabilities. The signal intensity of **S** decreases at 383 nm in the order **S**-Im > **S**-2-MeIm > **S**-2-Et-4-MeIm > **S**-N-MeIm, and the signal intensity of the adducts (at about 360 nm) increases in the same order, consistent with the thermodynamic results; CD spectra can quantify the strength of **S**-ligand interaction.

As for amino acid ester derivatives, the CD spectra of the **S**-ligand system are similar to those of the **S**-imidazole derivative system (figure 7). However, the selectivity of **S** towards the same amino ester with different configuration is different. The CD spectra of **S**-(*D*- and *L*-) PheOMe are shown in figure 8. *D*-PheOMe causes more apparent change in CD spectra than *L*-PheOMe. The discrepancy indicates a higher selectivity of SalenZn(II) towards *D*-PheOMe, which coincides with the order of binding constants.

3.3. *Molecular modeling*

Molecular modeling was performed in the Tripos force field as implemented in Sybyl 6.9 software on an SGI Indigo II workstation. The energy minimization was carried out with a gradient of 0.01 kcal mol^{-1}. The minimum energy conformation of **S** was obtained by the method of simulated annealing. On the basis of this conformation, the minimum energy conformations of **S** binding with the ligands were obtained by the same method. Quantum chemical calculations were performed by the method of Hatree–Fock at 6–31G level with Guassian 98 program package [19].

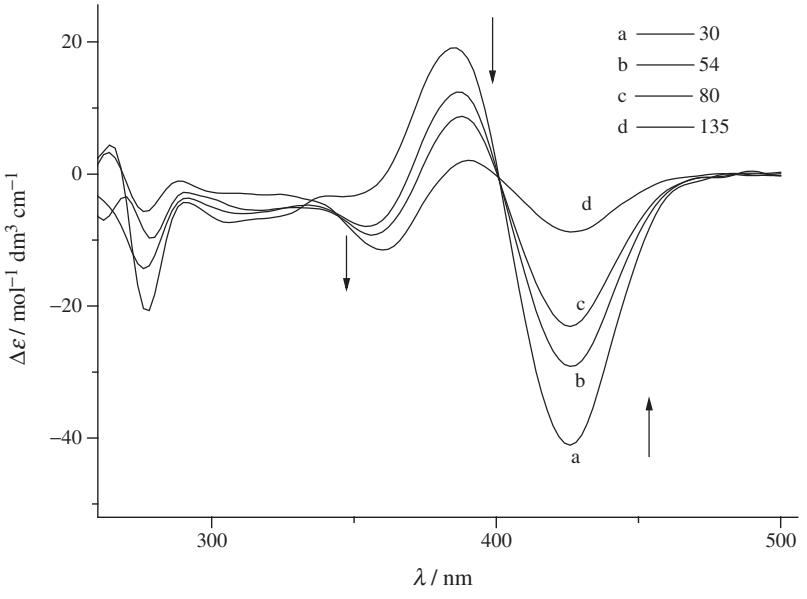

Figure 7. The CD spectra of **S**-*D*-PheOMe system (a–d are the concentration ratios of [ligand]/[**S**]).

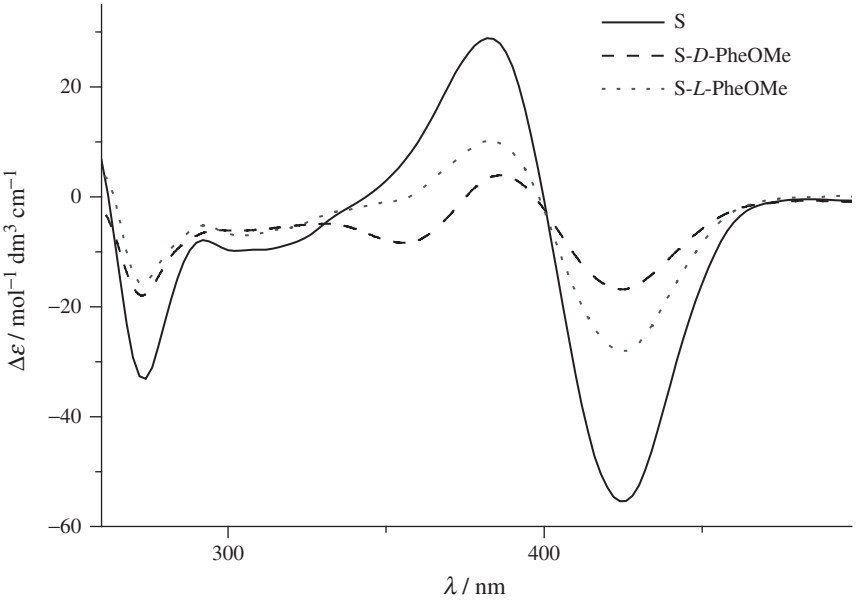

Figure 8. The CD spectra of **S**-(*D*- and *L*-) PheOMe system (the concentrations of *D*- and *L*-PheOMe are equivalent).

Figure 9 illustrates the minimum energy conformations of **S** (a), the adducts binding with Im (b) and with *D*-AlaOMe (c). The bond lengths of Zn–O, Zn–N, and Zn–N* (between **S** and the ligand) are listed in table 3. From the results it can be seen that the Zn–O bond length becomes longer after the adducts formed, indicating that

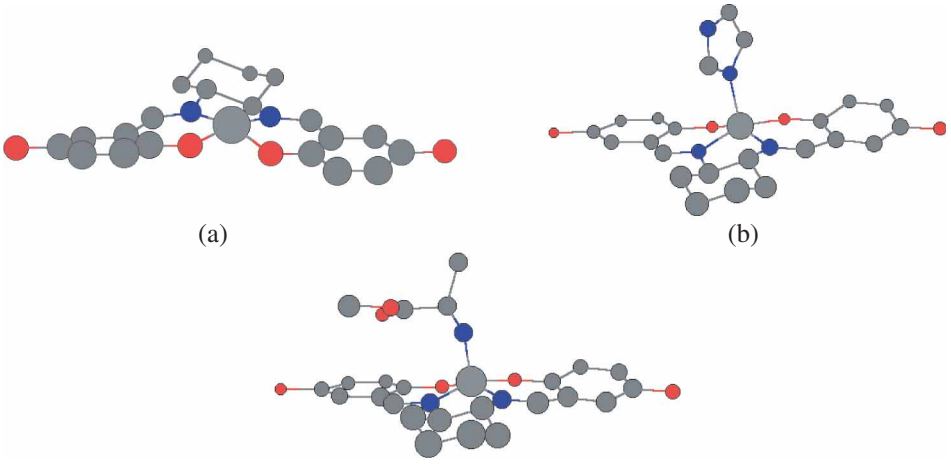

Figure 9. The minimum energy conformations of **S** (a) and the adducts binding with Im (b) and with *D*-AlaOMe (c).

Table 3. The bond lengths of Zn–O, Zn–N and Zn–N* (between **S** and the ligand).

Compounds	Zn–O1 (Å)	Zn–O2 (Å)	Zn–N1 (Å)	Zn–N2 (Å)	Zn–N* (Å)
S-Im	1.856	1.846	1.918	1.918	1.924
S-2-MeIm	1.860	1.850	1.922	1.924	1.932
S-EtMeIm	1.864	1.854	1.928	1.932	1.938
S-N-MeIm	1.866	1.856	1.932	1.936	1.944
S-*D*-AlaOMe	1.855	1.842	1.909	1.910	1.918
S-*L*-AlaOMe	1.852	1.842	1.912	1.911	1.919
S-*D*-PheOMe	1.859	1.850	1.916	1.916	1.924
S-*L*-PheOMe	1.859	1.849	1.920	1.922	1.926
S-*D*-ValOMe	1.861	1.854	1.919	1.918	1.925
S-*L*-ValOMe	1.860	1.852	1.919	1.919	1.928
S	1.843	1.829	1.901	1.901	

the zinc(II) of the adduct projects more from the plane of N–O–O–N than that of **S**. The variation is one of the reasons resulting in the changes of CD spectra. In addition, the stability of the adduct can be reflected through the Zn–N* bond length (between **S** and the ligand). The shorter the bond length, the more stable the adduct. The results listed in table 3 support the thermodynamic results.

Table 4 shows HOMO and LUMO energies of **S** and of the adducts. The energy of HOMO is negative, which indicates the adducts are stable. The energy difference ΔE_{L-H} of adducts are larger than that of **S**, which indicates the energy of electronic transitions have increased, so the absorption bands in UV-vis spectra of adducts are blue-shifted. The bigger the ΔE_{L-H}, the more stable the adduct [20]. The results listed in table 4 are consistent with those measured in UV-vis spectrophotometric titrations. In addition, ΔE_{D-L} are positive which indicates the adducts binding with *D*-amino acid ester are more stable than those with *L*-amino acid ester.

Table 4. HOMO and LUMO energies of S and of the adducts.

Compound	E_H(HOMO) (a.u.)	E_L(LUMO) (a.u.)	ΔE_{L-H}[a] (LUMO-HOMO) (a.u.)	ΔE_{D-L}[b] (a.u.)
S-Im	−0.23334	0.10192	0.33526	
S-2-MeIm	−0.23285	0.10108	0.33393	
S-EtMeIm	−0.23369	0.09645	0.33014	
S-N-MeIm	−0.22976	0.09773	0.32749	
S-*D*-AlaOMe	−0.23621	0.09838	0.33459	0.00333
S-*L*-AlaOMe	−0.23458	0.09668	0.33126	
S-*D*-PheOMe	−0.23413	0.09862	0.33275	0.00637
S-*L*-PheOMe	−0.23086	0.09552	0.32638	
S-*D*-ValOMe	−0.23767	0.09816	0.32774	0.00559
S-*L*-ValOMe	−0.23052	0.09440	0.32215	
S	−0.24068	0.08093	0.32161	

[a] $\Delta E_{L-H} = E_{LUMO} - E_{HOMO}$.
[b] $\Delta E_{D-L} = \Delta E_{L-H}$(**S**-*D*-amino acid ester) − ΔE_{L-H}(**S**-*L*-amino acid ester).

Acknowledgements

This work is supported by the National Nature Science Foundation (Nos. 20271030 and 20303009), the Tianjin Natural Science Foundation (No. 023604011).

References

[1] J.K. Nessan, J.L. Ivan, T.D. Cormac, M.D. Adrian, B. Claudine, G.G. Declan. *Tetrahedron Letters*, **43**, 2107 (2002).
[2] I.K. Rukhsana, H.K. Noor-ul, H.R. Sayed, S.T. Abdi, P. Patel, K. Iyer, V.J. Raksh. *Tetrahedron Letters*, **43**, 2665 (2002).
[3] B.M. Choudary, M.L. Kantam, B. Bharathi, R. Venkat, C.R. Chinta. *Jounal of Molecular Catalysis A: chemical*, **168**, 69 (2001).
[4] S. Bunnai, K. Tsutomu. *Tetrahedron Letters*, **42**, 8333 (2001).
[5] Y.N. Belokon, M. North, T.D. Churkina, N.S. Ikonnikov, V.I. Maleev. *Tetrahedron*, **57**, 2491 (2001).
[6] H. Nishikori, T. Katsuki. *Tetrahedron Letters*, **37**, 9245 (1996).
[7] M.A. Kwon, G.J. Kim. *Catalysis Today*, **87**, 145 (2003).
[8] S. Chang, J.M. Galvin, E.N. Jacobsen. *J. Am. Chem. Soc.*, **116**, 6937 (1994).
[9] E.N. Jacobsen, F. Kakiuchi, R.G. Konsler, J.F. Larrow, M. Tokunaga. *Tetrahedron Letters*, **38**, 773 (1997).
[10] E.N. Jacobsen, L. Deng, Y. Furukawa, L.E. Martinez. *Tetrahedron*, **50**, 4323 (1994).
[11] T. Mizatani, T. Ema, T. Tomita, Y. Kuroda, H. Ogoshi. *J. Am. Chem. Soc.*, **116**, 4240 (1994).
[12] F. Galsbol, P. Steenbol, S. Sondergaard. *Acta Chem. Scand.*, **26**, 3605 (1972).
[13] Y. Ma, Z.A. Zhu, R.T. Chen. *Thermochimica Acta.*, **171**, 223 (1990).
[14] N.D. Rose, R.S. Drago. *J. Am. Chem. Soc.*, **81**, 6138 (1959).
[15] Y.L. Zhang, W.J. Ruan, X.J. Zhao, H.G. Wang, Z.A. Zhu. *Polyhedron*, **22**, 1535 (2003).
[16] A. Wojtczak, E. Szlyk, M. Jaskolski, E. Larsen. *Acta. Chem. Scand.*, **51**, 274 (1997).
[17] J. Fujita, Y. Shimura. In *Spectroscopy and Structure of Metal Chelate Compounds*, K. Nakamoto, P.J. Mccarthy (Eds.), chapter 3, Wiley, New York (1968).
[18] E. Szłyk, S. Biniak, A. Surdykowski, I. Łakomska, M. Barwiołek. *Transition Met. Chem.*, **27**, 501 (2002).
[19] J. Frisch, G.W. Trucks, M. Head-Gordom, P.M.W. Gill, M.W. Wong, J.B. Foresman, B.G. Johnson, H.B. Schlegel, M.A. Robb, E.S. Replogle, R. Gompers, J.L. Anders, K. Raghavachari, J.S. Binkley, C. Gonzales, R.I. Martin, D.J. Fox, D.J. Defrees, J. Baker, J.J.P. Stewart, J.A. Pople, Gaussian 98, Gaussian. Inc. Pittsburgh, PA, 1998.
[20] D.E. Manolopoulos, J.C. May, S.E. Down. *Chem. Phys. Lett.*, **181**, 105 (1991).